Proceedings of the 11th ICPMG 2026
11th International Conference on Physical Modelling in Geotechnics
8-12 June 2026, Zurich, Switzerland

Moisture migration in unsaturated sandy soil around energy pile and its mechanical consequences: a model test study

G.H. Tang
Tongji University, Shanghai, China, TangGuohang@tongji.edu.cn

X.F. Ma, B.L. Ma, Y.H. Hu & H.H. Zhang
Tongji University, Shanghai, China

ABSTRACT: The influence of heat extraction during winter operation of energy piles on soil moisture migration and pile bearing capacity in unsaturated soils has long been a frequently overlooked critical issue. This study conducted a model test to simulate the winter heating mode of an energy pile in unsaturated sandy soil, quantifying the effects of heat extraction via a U-tube pile on the resulting soil temperature field and concomitant moisture migration. After the temperature and moisture fields reached a relative steady state, a vertical load was employed to obtain the pile's load-settlement curve. Results revealed that soil cooling induced by heat extraction altered moisture distribution patterns, causing moisture to accumulate around the cooler pile body. This local increase in water content subsequently impaired the geotechnical bearing capacity, leading to an approximately 18% increase in the in settlement of energy pile. This research enhances the understanding of unsaturated soil behavior under thermal loads imposed by energy pile operation, emphasizing the necessity to account for thermally driven moisture redistribution and its mechanical consequences in energy geo-structure design. The findings provide experimental validation for the thermo-hydro-mechanical coupling mechanisms specific to heating scenarios, offering a foundation for optimizing sustainable energy geo-structures and refining numerical models.

1 INTRODUCTION

Shallow geothermal energy (depth ≤ 200 m) is a widely available, stable renewable resource crucial for reducing building energy use (Moore & Simmons, 2013). Among the technologies harnessing this resource, the energy pile integrates heat exchange pipes of ground-source heat pump systems into building foundation piles, significantly enhancing the economic viability and spatial efficiency of geothermal systems (Liu et al., 2025).

The operational cycles of energy piles subject them to periodic temperature variations. This disrupts the initial thermal equilibrium of the surrounding soil, triggering complex thermo-hydro-mechanical (THM) coupled interactions that affect their long-term bearing performance (Fang et al., 2020; Lv et al., 2020). Temperature-controlled tests have been widely employed to investigate soil deformation under these coupled temperature-stress fields. For instance, saturated clays exhibit volumetric compressive strains up to 1.8% under thermal cycles, with the magnitude increasing with the plasticity index (Demars, 1982). In saturated sands, thermally-induced volumetric deformation is governed by the interplay between relative density and effective stress: at constant effective stress, deformation transitions from thermal contraction to expansion as relative density increases; conversely, at constant relative density, an increase in effective stress induces an opposite transition (Ng et al., 2016).

Shaft friction, vital to pile capacity, evolves complexly under thermal cycles. Temperature changes (5~60°C) minimally affect sand-concrete interface strength directly. However, heating causes volumetric contraction in saturated sands, exacerbated by lower normal stress and relative density (Rafai et al., 2025; Maghsoodi et al., 2019).

The scenario is further complicated in unsaturated soils. The heat exchange process in energy piles not only alters the temperature and stress fields but also drives moisture migration and redistribution, consequently modifying the intensity of capillary forces (Ghasemi-Fare and Basu, 2019; Bodas Freitas et al., 2021; Nazmabadi et al., 2022). These changes significantly impact the heat exchange efficiency and stability of energy piles (Han and Yu, 2020; Yang et al., 2020). Vapor migration in unsaturated soils under thermal and moisture gradients is considerable and intensifies with increasing gradient magnitude (Nakano et al., 1984). Eigenbrod and Kennepohl (1996), through freezing tests on coarse-grained soil, observed an increase in moisture content at the soil column surface from 6.6% to 11.1% due to temperature gradients. The seminal coupled heat and moisture transfer model for unsaturated soils was established by Philip and De Vries (1957), identifying moisture and temperature gradients as the primary drivers. This framework was later advanced by Thomas and He (1995) to develop a comprehensive THM coupling theory applicable to deformable unsaturated soils.

In summary, energy pile operation alters the surrounding soil's temperature and moisture fields, thereby influencing pile bearing behavior. Existing research, however, has focused primarily on thermal effects in saturated soils, often examining soil properties or interface behavior in isolation (Luo et al., 2019; Teng et al., 2019). The intrinsic mechanisms by which the coupled evolution of temperature and moisture in the unsaturated zone affects pile settlement and capacity remain inadequately understood.

This study aims to investigate these processes through a laboratory-scale physical model test, simulating the heat exchange of an energy pile under constant load in unsaturated sand subjected to a winter-like low-temperature boundary. The research focuses specifically on elucidating the patterns of temperature-driven moisture migration and its subsequent feedback effect on pile head settlement, thereby providing a theoretical basis for the safe design and performance assessment of energy piles in unsaturated ground.

2 MATERIAL AND METHODS

The model test was designed based on similarity theory to ensure that the physical phenomena observed in the model accurately reflect the actual behavior of a reference in-situ energy pile. The prototype energy pile was 2000 cm in length, 150 cm in diameter, made of C40 concrete, and embedded in a sandy soil stratum. It was equipped with a U-tube heat exchanger (inner diameter: 2.6 cm) through which heat carrier fluid circulated at 40 cm/s, under a pile head load of 880 kN.

A geometric similarity ratio of 1:40 was adopted between the model and prototype, adhering to stiffness similarity. Within this similitude system, the stress similarity constant and strain similarity constant were both set to 1, while the displacement similarity constant was 40. Consequently, the force similarity constant was derived as 1600, leading to a corresponding model pile head load of 550 N. This ensured consistency in stress distribution and deformation characteristics between the model and prototype.

For thermal similarity, the accuracy of the heat transfer process was maintained by preserving the similarity of the Péclet number (characterizing convective heat transfer) and the Fourier number (characterizing transient heat conduction). Simultaneously, the Reynolds number of the fluid flow inside the model pile's pipe was kept consistent with the prototype condition to ensure similarity in flow regime and heat transfer characteristics.

2.1 Soil properties and sample preparation

The particle size distribution of Fujian standard sand is uniform, and its matrix suction is relatively small. It is used as the test soil sample. The particle gradation curve and the soil-water characteristic curve are shown in Figure 1.

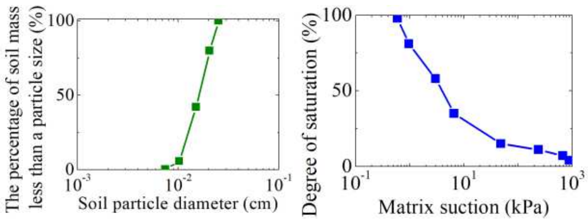

(a) Particle size distribution

(b) Soil water retention curve

Figure 1. Particle size distribution of the test soil.

The sandy soil had an average particle size (d_{50}) of 0.016 cm, a specific gravity (G_s) of 2.63, and an internal friction angle (φ) of 35°. The sandy soil was pluviated to a dry density of 1.55 g/cm^3 with an initial moisture content of 8% (S_r=30.18%), simulating a natural unsaturated sandy stratum (The degree of saturation (S_r) in this paper was calculated from the monitored gravimetric water content (ω), dry density, and specific gravity of soil solids.). To avoid the influence of gravity on moisture migration, rapid specimen preparation was essential. Therefore, a controlled pluviation method was adopted: the sand (with an initial water content of 8%) was first mechanically sieved to break up initial clumps and then dispersed using a wide-mouth spreader head. Low-amplitude, high-frequency vibration was briefly applied to the spreader head at the onset of pluviation to overcome slight agglomeration of the moist sand. After deposition, only minor surface leveling was performed (without compaction). The final soil sample height was 90 cm, achieving a relative density of approximately 65%, indicative of a medium-dense state. The measured thermal conductivity and specific heat capacity of the soil were 0.35 W/(m·K) and 920 J/(kg·K), respectively.

2.2 Model pile

The model energy pile was constructed from C40 concrete, with a length of 50 cm and a diameter of 3.75 cm. The measured concrete properties included a compressive strength of 40 MPa, an elastic modulus of 29.7 GPa, and a linear expansion coefficient of 1.0×10^{-5} °C^{-1}. A U-shaped PVC pipe (inner diameter: 1.5 cm) was embedded in the pile, with the outer pipe wall positioned 0.3 cm from the pile surface. Pure water served as the heat carrier fluid, circulated at a velocity of 70 cm/s (corresponding to a Reynolds number of 10500, indicating turbulent flow). The inlet temperature was set to 5°C to simulate winter operating conditions.

2.3 Test setup

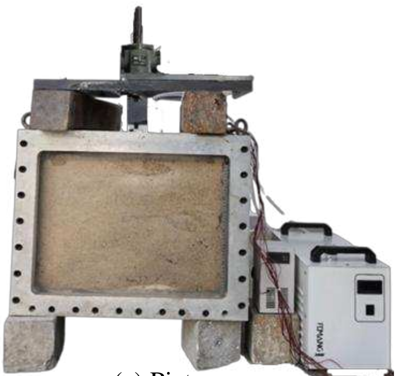

(a) Picture

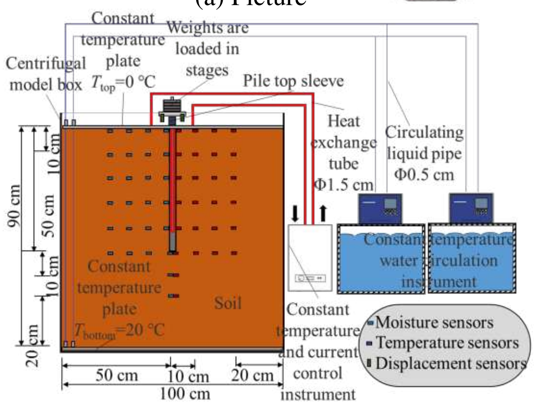

(b) Schematic diagram

Figure 2. Schematic diagram of the model test setup.

The model container was insulated with 5 cm-thick foam boards on its sides to provide adiabatic boundary conditions. The temperature control system consisted of a bottom constant-temperature plate (maintained at 17°C to simulate the ground temperature at 3600 cm depth) and a top constant-temperature plate (maintained at 0°C to simulate the winter surface temperature). The top plate featured a custom-made central opening to accommodate the model pile, as shown in Figure 2. The container and loading system were leveled using a spirit level prior to placement and loading, with the base support blocks serving solely as rigid spacers to ensure stable loading conditions.

This system was activated for 120 hours prior to pile testing to establish a stable linear temperature distribution within the soil. The instrumentation system (Figure 2) included:

(1) Temperature field: A total of 24 T-type thermocouples were installed at distances of 0 cm, 10 cm, 20 cm, and 30 cm from the pile surface, distributed along the pile depth at 10 cm intervals. Two additional thermocouples were placed 10 cm and 20 cm beneath the pile tip.

(2) Moisture field: Twenty-six Time-Domain Reflectometry (TDR) sensors were positioned at locations corresponding to the thermocouples to measure volumetric moisture content.

(3) Displacement: Pile head settlement was monitored in real-time using a Linear Variable Differential Transformer (LVDT) with an accuracy of ±0.001 cm. They were mounted on a rigid reference frame independent of pile movement.

2.4 Test procedure

The test was conducted in the following sequence:

(1) The top and bottom temperature control systems were activated for 120 hours to establish a stable linear temperature field in the soil. The initial distributions of the temperature and moisture fields were recorded.

(2) A vertical load of 550 N was applied to the model pile head in increments of 50 N. Each load increment was maintained for 0.5 hour, and the load-settlement curve was recorded.

(3) The full load was maintained for 48 hours to monitor the creep settlement of the model pile under non-operational conditions.

(4) The energy pile's heat exchange system was activated, circulating fluid at an inlet temperature of 5°C continuously for 120 hours. Data for temperature, moisture content, and pile head displacement were automatically acquired at a frequency of 1 minute throughout this period.

The entire test was conducted in a constant-temperature laboratory environment maintained at 20 ± 2°C to minimize external interference.

3 RESULTS AND DISCUSSION

After 120 hours of activating the top and bottom constant-temperature systems, the distributions of the temperature and moisture fields are shown in Figure 3, which is presented as providing the initial soil state before pile operation, established after 120 hours of boundary temperature control, for reference

Figure 3(a) shows a linear increase in temperature from the top to the bottom. The minimal data variation (standard deviation < 0.03, hence error bars are nearly invisible) between temperature sensors at the same depth confirms the effectiveness of the boundary temperature control and insulation, indicating heat conduction was the dominant process. Figure 3(b) reveals a significant moisture redistribution induced solely by the vertical temperature gradient over 120 hours. The moisture content increased near the top cold source (0°C), rising from 8% to 13.57% (S_r: 30.19~50.20%) at the top, demonstrating upward moisture migration driven by the temperature gradient. Conversely, the moisture content between depths of 40~60 cm fell below the initial value, indicating moisture migration upwards or gravitational drainage downwards from this zone. A slight moisture increase around 70 cm depth further confirmed downward seepage due to gravity. Therefore, the distribution in Figure 3(b) is a coupled steady state of "driven by the combined effect of temperature gradient and gravity," which is completely different from a distribution formed solely by gravitational drainage.

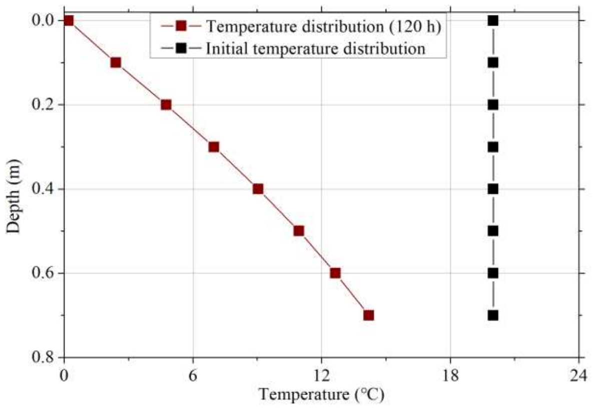

(a) Temperature in the soil is distributed with depth

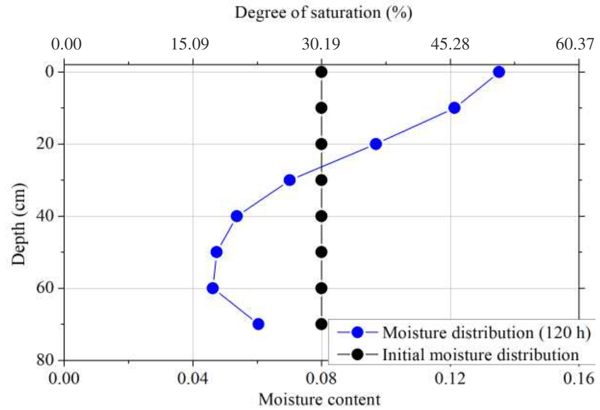

(b) Moisture content in the soil is distributed with depth

Figure 3. Distribution of temperature and moisture content with soil depth.

Following the activation of the energy pile's heat exchange system, the evolution of the soil temperature and moisture fields was monitored (inlet temperature: 5°C) for 120 hours, the temporal and spatial evolution of temperature and moisture content at different horizontal distances from the pile is presented in Figure 4 ((a): 0 cm; (b): 10 cm; (c): 20 cm; (d): 30 cm. Lines represent data at 1 h (black), 8 h (red), 24 h (blue), 72 h (purple), and 120 h (green) of operation). (Note that the '1 h' profile in Figure. 4 (a) and (b) corresponds to 1 hour after pile thermal activation and thus differs from the initial state in Figure 3(a) and (b).)

Figure 4(a) clearly illustrates the dynamic disturbance of the initial linear temperature field by the operating energy pile (acting as an internal cold source). Temperature changes are faster and larger near the pile horizontally. At the soil surface (0 cm depth), changes are minor due to the 0°C boundary. Deeper along the pile, temperatures drop rapidly, altering the profile. This effect weakens with distance, becoming negligible at 30 cm. The most rapid changes occur in the first 1~24 hours, slowing and stabilizing by 72~120 hours. The system reaches a new equilibrium, transforming the one-dimensional field into a two-dimensional field centered on the pile.

Figure 4(b) directly reveals the patterns of thermally-driven moisture migration.

Upper Pile Section: This zone was initially colder than the pile temperature (5°C). Pile operation warmed the adjacent soil, creating a temperature gradient driving moisture away from the warmer pile, causing a significant decrease in moisture content nearby (e.g., at 10 cm depth, from 11.73% to 9.30% (S_r: 44.26~35.09%)). Correspondingly, moisture content increased at farther horizontal distances (e.g., at 20 cm horizontal distance and 0 mm depth after 72 h, from 13.81% to 14.73% (S_r: 52.11~55.58%)).

Lower Pile Section/Base: This zone was initially warmer than the pile. Pile operation cooled this area, forming a local cold zone that drew moisture towards the pile, leading to a significant increase in moisture content nearby (e.g., at the pile periphery and 0 mm depth after 120 h, from 6.03% to 12.92% (S_r: 22.75~48.75%)). Additionally, moisture migrating downward from upper and middle sections likely accumulated below the pile tip due to gravity, making the moisture increase in the base region a result of competing mechanisms (temperature gradient, gravity, initial conditions).

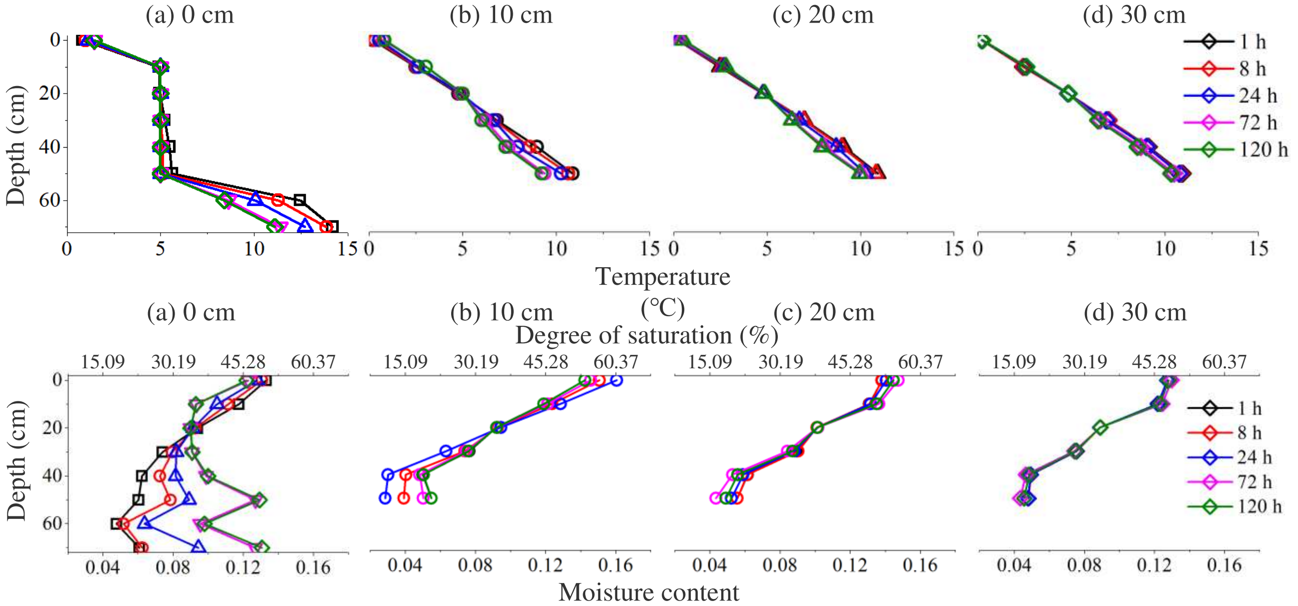

Figure 4. Distribution of temperature and moisture content with depth at different horizontal distances and times.

The energy pile, as an internal thermal disturbance, disrupted the initial moisture equilibrium, driving a two-dimensional redistribution and creating a heterogeneous moisture content field around the pile, which is crucial for pile-soil interaction.

Furthermore, the temperature and moisture changes in the soil near the top of the energy pile, which constitutes the bearing layer, are the main factors influencing the bearing characteristics of the energy pile. During the operation of the energy pile, the changes in temperature and moisture of the soil near the pile top are shown in Figure 5.

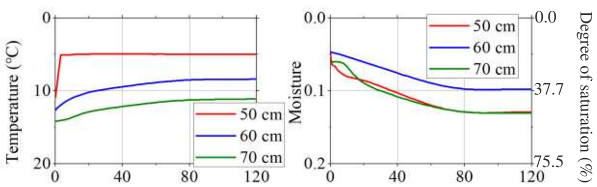

(a) Soil temperature below the pile tip

(b) Soil moisture below the pile tip

Figure 5. Changes in temperature and moisture of soil near the pile tip after energy pile operation.

During the 120-hour operation period, the temperature and moisture content at 0 cm, 10 cm, and 20 cm (corresponding to soil depths of 50 cm, 60 cm, and 70 cm, respectively) below the pile tip decreased (Figure 5). This directly confirms the role of the pile base as a persistent cold sink, which is the thermodynamic driver for the observed moisture accumulation in that region.

It could have quantified the outlet temperature by analyzing the change in the internal energy of the soil within the thermal influence zone. After 120 hours of operation, the cylindrical soil volume surrounding the pile (radius ≈ 35 cm, height ≈ 75 cm) is the volume thermally affected by the pile operation. It was divided into several concentric cylinders. The temperature change recorded by each sensor after 120 hours (ΔT_{soil}) represents the average temperature change for its corresponding representative soil cylinder volume. The prototype total heat extracted can be calculated by: $Q_{prototype} = \sum C_F \cdot (1-\phi)\rho_s c_s \cdot V_{soil} \cdot \Delta T_{soil} = -83548.16kJ$, where ϕ is porosity; ρ_s is soil particle density; c_s is soil specific heat (920 J/(kg·K)); V_{soil} is the volume of the thermally affected soil cylinder; C_F is established force similarity constant (1600). The associated fluid temperature rise for the prototype is then: $\Delta T = T_{out} - T_{in} = Q_{prototype} / (\dot{m} \cdot c_p \cdot t) = 2.18℃$, where, $\dot{m}$ is the mass flow rate, $\dot{m} = \rho \cdot A \cdot v$; ρ is the fluid density; A is the cross-sectional area of the U-tube; v is the fluid velocity; t is time; c_p is the specific heat capacity of the fluid.

This gives an outlet temperature of 7.18°C.

Figure 6(a) shows the load-settlement curve during incremental loading (50 N increments, 0.5 hour) to 550 N applied before pile operation. Figure 6(b) presents the creep settlement during the subsequent 48-hour period under sustained load without operation, and the additional settlement during the 120-hour operation period with a 5°C inlet temperature, induced by changes in the soil's temperature and moisture fields.

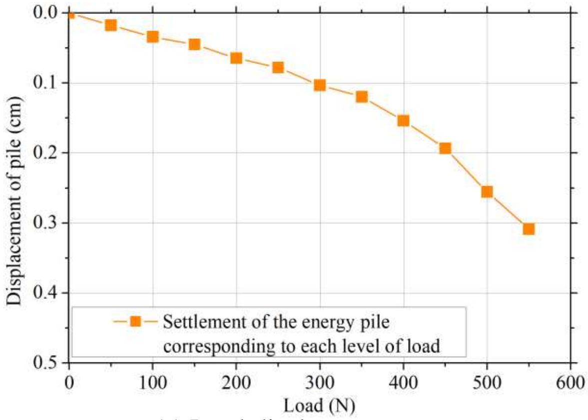

(a) Load-displacement curve

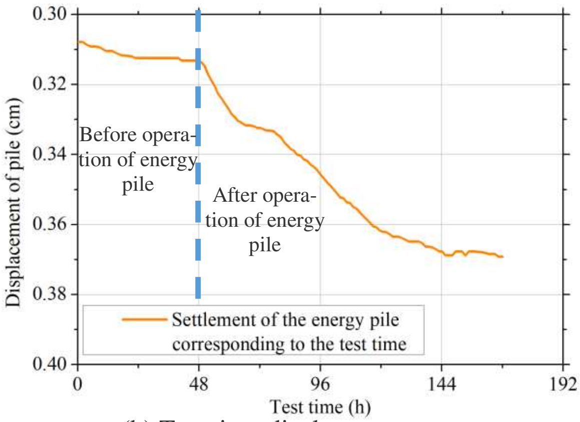

(b) Test time-displacement curve

Figure 6. Load-settlement curve during incremental loading, creep settlement and thermo-hydraulically-induced settlement during energy pile operation.

Figure 6(a) reflects the initial mechanical performance of the model pile under a stable linear temperature distribution. The absence of a sharp yield point in the curve suggests progressive failure characteristics, consistent with the behavior of friction piles in sand. The pile did not undergo overall shear failure at 550 N, but its capacity was approaching the ultimate state (indicated by the increasing rate of displacement).

Figure 6(b) illustrates the pile settlement under thermo-hydro-mechanical coupling effects.

Stage I (mechanical creep settlement): Before energy pile operation, the pile head settlement increased slowly with time over 48 hours under sustained load—a typical soil creep process—with a minor magnitude (only 0.005 cm).

Stage II (thermally-induced settlement): Over the subsequent 120-hour operational period (48~168 h), the settlement increased by approximately 0.056 cm , which was much higher than that in Stage I. Therefore, the additional settlement (Δs) is a direct consequence triggered by the energy pile's operation, not a continuation of mechanical creep. The pile operation (cold fluid circulation) created a new temperature field centered on the pile, exerting a heating effect relative to the low-temperature surface boundary and a cooling effect relative to the constant-temperature zone deeper in the soil. Consequently, thermal expansion and contraction occur simultaneously. Notably, the thermal expansion of the pile itself might even cause uplift, as reported by (Cen & Xia, 2026; Rafai et al., 2025). Specifically, energy piles can generate upward negative shaft resistance due to thermal expansion during heating, causing the pile to move upward relative to the soil. However, our experimental result shows significant settlement after pile operation. This clearly indicates that this additional settlement is not governed by the pile's thermal expansion/contraction.

The operation cooled the soil around the pile base (Figure 4(a)), driving moisture towards it (Figure 4(b)). After 120 hours, water content around the pile increased from 9.01% to 10.41% (S_r: 34.00~39.28%), and below the pile tip from 5.42% to 11.41% (S_r: 20.45~43.05%). The pile response is influenced by this moisture accumulation through multiple interacting effects, including: locally reduced effective stress and inter-particle bonding in unsaturated zones (wetting-induced rearrangement); increased unit weight in wetted zones; reduced bearing resistance due to localized increases in water content.

4 CONCLUSIONS

This study reveals a critical yet often overlooked mechanism governing the behavior of energy piles in unsaturated sandy soil during winter operation: temperature-gradient-driven moisture redistribution around the pile is the dominant factor controlling its thermo-mechanical response, particularly the additional settlement. The main conclusions are as follows:

(1) In unsaturated sandy soil, the operation of an energy pile transforms the initial one-dimensional temperature field into a complex two-dimensional field centered on the pile, with a radial thermal influence extending approximately 30 cm (about 8 times the pile diameter). This altered temperature field, combined with gravitational drainage, drives directional moisture migration.

(2) The temperature in the upper and middle sections of the pile shaft becomes higher than that of the surrounding soil, causing heat to diffuse outwards and drive moisture away from the pile, resulting in desiccation of the adjacent soil. Conversely, the pile base and lower section act as a cold sink, strongly drawing moisture towards and accumulating it in the underlying bearing layer. This significant wetting directly causes soil softening and a reduction in

effective stress, which is the fundamental reason for the substantial additional settlement (approximately 18%) observed under constant mechanical load.

ACKNOWLEDGEMENTS

The authors are grateful for the Fundamental Research Funds for the Central Universities [No. 22120230077 and 2023-2-ZD-01] in China.

REFERENCES

Bodas Freitas, T. M., Zito, M., Bourne-Webb, P. J., and Salciarini, D. (2021). Thermal performance of seasonally, thermally-activated floating pile foundations in a cohesive medium. *Engineering Structures*, 243: 112588. https://doi.org/10.1016/j.engstruct.2021.112588

Cen, D., and Xia, C. (2026). Review on heat transfer and thermo-mechanical behaviour of energy geostructures. *Underground Space*, 26: 36-81. https://doi.org/10.1016/j.undsp.2025.06.003

Demars, K. R. (1982). Soil volume changes induced by temperature cycling. *Canadian Geotechnical Journal*, 19(2): 188-194. https://doi.org/10.1139/t82-021

Eigenbrod, K. D., and Kennepohl, G. J. A. (1996). Moisture Accumulation and Pore Water Pressures at Base of Pavements. *Transportation Research Record*, 1546(1): 151-161. https://doi.org/10.1177/0361198196154600117

Fang, J., Kong, G., Meng, Y., and Yang, Q. (2020). Thermomechanical behavior of energy piles and interactions within energy pile-raft foundations. *Journal of Geotechnical and Geoenvironmental Engineering*, 146(11): 04020079. https://doi.org/10.1061/(ASCE)GT.1943-5606.0002333

Ghasemi-Fare, O., and Basu, P. (2019). Coupling heat and buoyant fluid flow for thermal performance assessment of geothermal piles. *Computers and Geotechnics*, 116: 103211. https://doi.org/10.1016/j.compgeo.2019.103211

Han, C. J., and Yu, X. (2020). Analyses of the thermo-hydro-mechanical responses of energy pile subjected to non-isothermal heat exchange condition. *Renewable Energy*, 157: 150-163. https://doi.org/10.1016/j.renene.2020.04.118

Liu, X., Zhang, G., Liu, Y., and Li, Q. (2025). Investigation on energy piles with phase change material backfill used for cold energy storage and extraction for substation cooling via field tests. *Journal of Energy Storage*, 135: 118411. https://doi.org/10.1016/j.est.2025.118411

Luo, T., Qu, X., Wang, N. D., and Zhang, J. Z. (2019). Pot-cover Effect and its prevention: An experimental study in the field. *Cold Regions Science and Technology*, 167: 102845. https://doi.org/10.1016/j.coldregions.2019.102845

Lv, Z., Kong, G., Liu, H., and Li, C. (2020). Effects of soil type on axial and radial thermal responses of field-scale energy piles. *Journal of Geotechnical and Geoenvironmental Engineering*, 146(11): 06020018. https://doi.org/10.1061/(ASCE)GT.1943-5606.0002368

Maghsoodi, S., Cuisinier, O., and Masrouri, F. (2019). Thermal effects on the mechanical behaviour of the soil-structure interface. *Canadian Geotechnical Journal*, 57(1): 32-47. https://doi.org/10.1139/cgj-2018-0583

Nakano, Y., Tice, A. R., and Oliphant, J. L. (1984). Transport of water in frozen soil III: experiment on the effects of ice content. *Advances in Water Resources*, 7(1): 28-34. https://doi.org/10.1016/0309-1708(84)90027-7

Nazmabadi, R., Asgari, B., and Hakkaki-Fard, A. (2022). On the thermal performance enhancement of spiral-coil energy piles with a thermal recovery system. *Energy and Buildings*, 269: 112240. https://doi.org/10.1016/j.enbuild.2022.112240

Ng, C. W. W., Wang, S. H., and Zhou, C. (2016). Volume change behaviour of saturated sand under thermal cycles. *Géotechnique Letters*, 6(2): 124. https://doi.org/10.1680/jgele.15.00148

Philip, J. R., and De Vries, D. A. (1957). Moisture movement in porous materials under temperature gradients. *Eos, Transactions American Geophysical Union*, 38(2): 222-232. https://doi.org/10.1029/TR038i002p00222

Rafai, M., Salciarini, D., and Vardon, P. J. (2025). Energy pile displacements due to cyclic thermal loading at different mechanical load levels. *Acta Geotechnica*, 20: 3067-3086. https://doi.org/10.1007/s11440-025-02556-4

Rafai, M., Tang, A. M., Badinier, T., de Sauvage, J., and Salciarini, D. (2025). Effect of thermal cycles on sand-concrete interface under constant shear stress. *Canadian Geotechnical Journal*, 62(5): 1-16. https://doi.org/10.1139/cgj-2024-0163

Teng, J. D., Shan, F., He, Z. Y., and Liu, S. Y. (2019). Experimental study of ice accumulation in unsaturated clean sand. *Géotechnique*, 69(3): 251-259. https://doi.org/10.1680/jgeot.17.P.208

Thomas, H. R., and He, Y. (1995). Analysis of coupled heat, moisture and air transfer in a deformable unsaturated soil. *Géotechnique*, 45(4): 677-689. https://doi.org/10.1680/geot.1995.45.4.677

Yang, W. B., Zhang, L. J., Zhang, H., and Lu, X. L. (2020). Numerical investigations of the effects of different factors on the displacement of energy pile under the thermo-mechanical loads. *Case Studies in Thermal Engineering*, 21: 100671. https://doi.org/10.1016/j.csite.2020.100711